Design of HIFU CMUT Arrays for Treatment of Liver and Renal Cancer

Serena H. Wong[*], Arif Sanli Ergun[*], Goksen G. Yaralioglu[*], Omer Oralkan[*], Mario Kupnik[*], Kim Butts Pauly[†], B.T. Khuri-Yakub[*]

[*] *Department of Electrical Engineering, Stanford University, Stanford, CA 94305-9505*
[†] *Department of Radiology, Stanford University School of Medicine, Stanford, CA 94305-5105*

Abstract. We present the development of a capacitive micromachined ultrasonic transducer (CMUT) array for noninvasive focused ultrasound ablation of lower abdominal cancers under MR-guidance. While piezoelectric transducers have been traditionally used for HIFU, recent advances in CMUT design have made them highly competitive. Not only are CMUTs cost effective, they allow fabrication flexibility and advantages in efficiency and bandwidth. Current imaging CMUTs have shown capability of HIFU operation through high power and continuous wave operation. In this paper, we will present the development of CMUT membranes designed specifically for HIFU. These membranes are piston-like membranes fabricated by placing a thick layer of silicon or gold at the center of the membrane. The width of the piston layer is usually 60-85% of the membrane width and allows the membrane mass and elasticity to be controlled independently. It also increases the average displacement and average output pressure of the membrane. We patterned these CMUT membranes into an 8 element, 3.5 cm concentric array. We simulated the heating patterns of this array to show it is capable of producing lesions of 5 mm in diameter within 20-30 seconds, which can be imaged using our MR detection software.

Keywords: MR-guided HIFU, CMUT
PACS: 43.38.Hz, 87.54.Hk

INTRODUCTION

Cancers of the upper abdomen cause great mortality and morbidity in the US. Such cancers include colorectal cancer metastic to the liver and hepatocellular carcinoma. Resection has been shown to greatly increase 5-year survival rate among hepatic cancer patients [1]. Unfortunately, only 20% of patients are suitable for resection. For the remaining patients, a potentially curative non-invasive treatment option would present a great advance. We propose such a system consisting of high intensity focused ultrasound (HIFU) probe guided by MRI temperature maps.

While piezoelectric transducers have been traditionally used for HIFU, CMUTs have recently shown competitive performance. In last year's conference, we showed that typical imaging CMUTs could produce output pressures in excess of 1MPa peak to peak and demonstrated continuous wave (CW) operation. In this year's paper, we will show the design and simulation of piston CMUT membranes specifically designed for HIFU applications. We will also present the design and simulation of an

CP911, 6^{th} *International Symposium on Therapeutic Ultrasound*
edited by C.-C. Coussios and G. ter Haar

concentric array that produces a 5 mm diameter necrosis region after 20 seconds, which can be imaged effectively under MR-guidance.

CMUT MEMBRANE SIMULATIONS

Since non-invasive HIFU needs to penetrate through thick tissue, we designed our CMUT membranes to have lower center frequencies between 1-3 MHz. The frequencies were low enough to aid penetration of ultrasound to these depths, but high enough for tight enough focusing of the array's beam. Since HIFU depends on the power gain of the array design, a surface output pressure of 1.5-2.5MPa peak to peak output pressure will be adequate to achieve the intensities necessary for ablation.

These new membrane designs are characterized by their piston-like behavior. The piston is created by fabricating a thick mass in the center of the membrane, either by electroplating a heavy gold electrode or by creating a thick layer of silicon using a double silicon wafer bonding process [2]. The piston enables the mass and elasticity of membrane to be controlled independently. Additionally, most of the membrane moves in-sync and displaces by the same amount; this increases the average membrane deflection for a given gap height, thereby increasing the output pressure. Though the extra mass and stiffness causes the transducer's bandwidth to decrease, for HIFU applications, excitation is at a single frequency, so the decrease in bandwidth does not negatively affect the transducer's performance.

Simulation Methods

Designs were modeled in ANSYS (ANSYS, Inc, Canonsburg, PA) assuming constant 37C throughout the structure and no initial stress in the materials. The CMUT oxide, silicon, and metals were modeled using PLANE42 elements (Fig.1). Circular membranes were simulated with axisymmetric symmetry, while rectangular membranes were simulated with planar symmetry and assumed to be infinite in length. Previous experiments have shown that rectangles with a width/length aspect ratio greater than 4:1 approximate infinite rectangles. A non-attenuating, non-absorbing water column of FLUID29 elements three wavelengths high was constructed on top of the CMUT, and an absorbing boundary was placed three wavelengths away from the surface. The pressure was measured half a wavelength away from the surface and averaged. Since the FLUID29 elements were non-absorbing, the average pressure calculated is the equivalent to the average surface pressure.#

Results and Discussion

Designs of several widths, two membrane thicknesses, two gap heights, and different geometries have been selected for fabrication. These designs have center frequencies ranging from 1-4 MHz and output pressures ranging from 0.75 MPa peak to peak to greater than 2 MPa peak to peak. An example response is shown in Fig.2. With these pressure levels, we will be able to use these membranes within the concentric array to effectively heat and ablate liver tissue.

ANSYS models

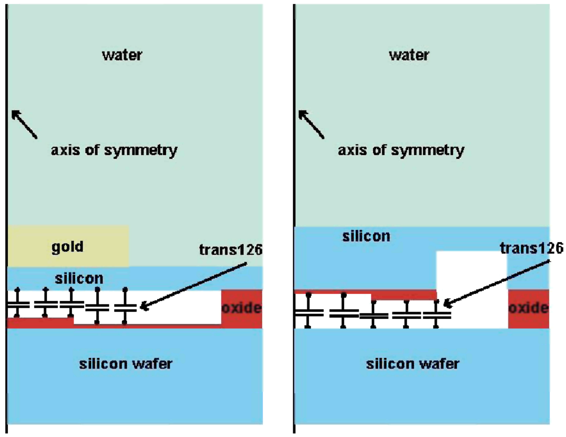

FIGURE 1. ANSYS models used to simulate the two types of piston transducers. (Left) One design of piston CMUTs uses the typical wafer bonding or silicon nitride processes to fabricate the membrane. In the final step, a thin layer of seed gold is deposited on the membrane by the lift-off photolithography process. Electroplating or electroless gold plating is then used to deposit a thick layer on the membrane surface in specifically designated spots, as defined by the gold seed layer lithography. (Right) A double wafer bonding process can also be used to fabricate a thick layer of silicon on the bottom side of the membrane [2].

Simulated Responses in ANSYS

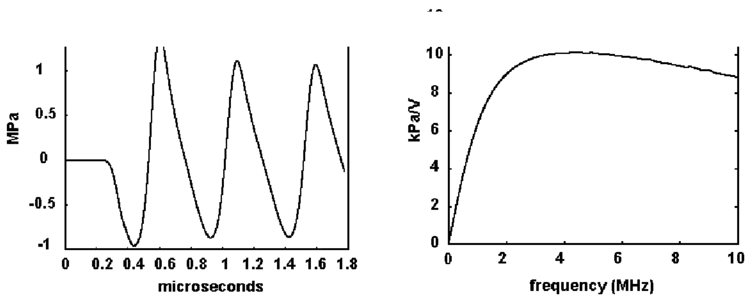

FIGURE 2. Example responses of transient pressure output (left) and harmonic response (right) of a typical silicon piston design. This design has a one micron membrane thickness and a piston thickness of 5 times the membrane thickness.

The best designs have piston widths between 60-85% of the membrane width and a piston thickness of about 5 times the thickness of the membrane. This piston width allows a flatter, larger, more piston-like membrane while still keeping a reasonable collapse voltage and good separation of elasticity and mass. If the piston width were to increase to almost the full width of the membrane, the additional thickness at the edge would add to the stiffness of the membrane. The piston thickness that was needed to keep the membrane relatively flat and piston-like was highly dependent on the elasticity of the membrane, which depended on the membrane thickness and membrane width. In general, a thickness of about 5 times the membrane thickness produced a relatively piston-like response.

Gold piston designs showed slightly higher output pressures and narrower bandwidth. This is because gold is much denser than silicon and will add more mass to the membrane. However, since the Young's modulus of gold is smaller than that of silicon, it produces a smaller effect on the stiffness of the membrane. This means that gold piston designs are easier to design for lower frequencies with smaller bandwidths and higher pressures.

The major limitation of the devices was found to be the voltage that could be applied to the device before the materials, especially the silicon oxide insulation layer, broke down. For a given gap height, larger applied voltages yield a larger electric field in the gap, which yield a larger pressure.

We are currently fabricating the silicon piston designs using a process similar to the double wafer bonding process developed previously by our group [2]. The gold piston process is currently under investigation since the thickness of gold required is such that electroplating or electroless plating is required. This step complicates some levels of the processing and is currently being investigated.

TRANSDUCER ARRAY BEAM PROFILE AND HEATING SIMULATIONS

We patterned the CMUT membrane designs described above into a transducer array designed for non-invasive HIFU ablation of liver tumors. This transducer array will be used on a moveable probe by the surgeon to apply therapy. Since the lateral motion of the transducer can be controlled by the surgeon, we chose to develop an concentric ring array that can only dynamically change the depth of focus. For use on the liver, we aimed to focus 3-5 cm deep within the tissue for a preliminary design. The desired burn spot size should be larger than about 2 mm in diameter, since MR thermometry technique has pixel size of approximately 0.1 cm and a TR of 167 ms [3,4].

We designed a prototype, 2 MHz, concentric equal-area, square transducer (Figure 1) with outer side length of 3.5 cm. Though a concentric circular design would increase the output pressure at the focus, for this quick prototype, we chose a square shape, which makes mask design and layout easier. In future designs, we will move to a circular even hexagonal design.

Simulation Methods

We used Huygen's principle [5], which assumes an array to be a collection of spherical sources, to calculate the beam profile of our array (Fig. 3). The phases applied to each element [6] focused the array beam at 4 cm. We assumed an attenuation of liver tissue of 0.4dB/cm/MHz [7].

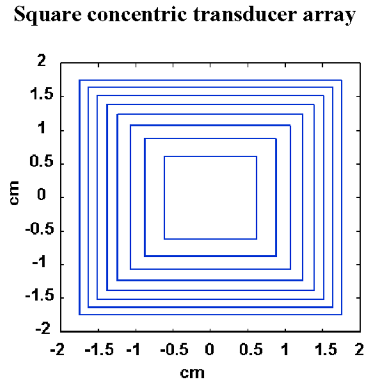

FIGURE 3. We designed a 2MHz square concentric, 8 element, equal element transducer array 3.5 cm in width for noninvasive HIFU treatment of liver tumors.

To determine the necrosis time and lesion size, we used the Pennes Bioheat Equation to calculate the temperature in a homogeneous region of liver tissue over time. We then used the Separato-Dewey Equation [8] to determine the necrosis region.The Pennes Bioheat Equation is given by

$$\rho c \frac{\partial T}{\partial t} = \nabla(k\nabla T) + \rho_b c_b w_b (T_a - T) + q_m , \tag{1}$$

where ρ is the density of liver, c is the conductivity of liver, k is the conduction coefficient of liver, ρ_b is the density of blood, c_b is the conductivity of blood, w_a is the perfusion coefficient, T_a if the bodies ambient temperature (37 C) and T is the temperature as a function of time. q_m refers to heat introduced into the tissue by the ultrasound, which is given by $2*\alpha*$Intensity. The intensity is given as the P_{peak}^2/Z, where P_{peak} is the pressure derived from our beam profile calculations.

We solved this PDE by calculating the second derivative of temperature with regard to space at each time point. Then at each point in space, we can solve an ODE to reach the successive time point.

To determine the necrosis threshhold, we used the cumulative equivalent minutes at 43 C, given by the equation

$$CEM_{43} = \sum_{t=0}^{t=tfinal} R^{(43-T(t))} \Delta t , \tag{2}$$

where T(t) is the temperature at a particular location in space as a function of time, which we calculated using the Pennes Bioheat Equation. Δt is the time step and t_{final} and $t_{initial}$ are the final and initial times, respectively. The constant R=0.25 if T(t) < 43 and R=0.5 if T(t) > 43. Necrosis of liver tissue is empirically determined at 240 equivalent minutes at 43 C [8].

Results and Discussion

From our pressure beam profile calculations we see that the –6dB contour is about 2 mm by 2mm by 7.5 mm. The additional lobes seen around the main lobe are caused by the square the shape of the transducer since the phase difference of the points on the same square ring vary by quite a bit. As the transducer becomes more circular, these lobes disappear. The power gain of this array is 15, whereas the power gain of a circular ring array is 36. In our simulations, we assumed the output at the transducer's surface was 1MPa peak pressure from our CMUT membrane designs to determine the pressure at points throughout the tissue sample.

Beam profiles

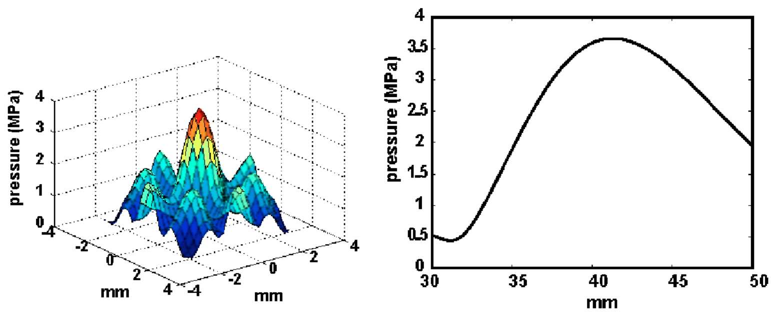

FIGURE 4. (left) pressure profile at the focal plane (4 cm) of our concentric array. (right) axial pressure profile.

Using the heating and necrosis equations, we determined the temperature and cumulative equivalent minutes at each point in the tissue over a 20 second time period. After about 20 seconds, a lesion of 5 mm in diameter should be formed at the focal point; the evolution of this region over time can be observed by MR imaging methods [3,4] (Fig.5).

Temperature and Necrosis Thresholds

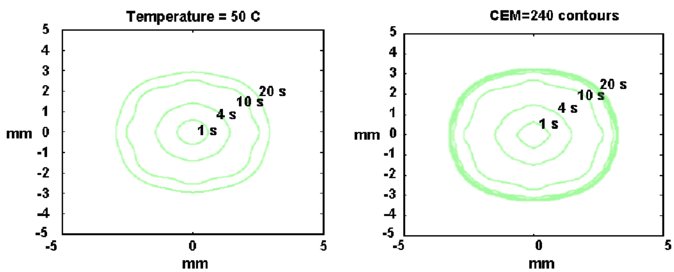

FIGURE 5. Contour of the 50C contours (left) in our tissue sample simulated from 0-20 seconds after HIFU application. Cumulative equivalent minutes of 240 contours (right) in the tissue that determine the region of tissue necrosis over time.

CONCLUSIONS

CMUT membrane designs and a transducer array with sufficient power gain has been simulated and designed for MR-guided HIFU ablation of liver tumors. This CMUT membrane design is a piston-like design that outputs 2 Mpa peak to peak pressure. With this output pressure and the transducer array configuration, a region of 5 mm in diameter can be ablated in 20 seconds. These designs are being fabricated and are currently being tested.

ACKNOWLEDGEMENTS

This research is supported under NIH R01 CA77677, R01 CA 121163.

REFERENCES

1. American_Cancer_Society, Cancer Statistics. 2004.
2. Huang, Y.L., et al., *Fabricating capacitive micromachined ultrasonic transducers with wafer-bonding technology*. Journal of Microelectromechanical Systems, 2003. 12(2): p. 128-137.
3. Rieke, V., et al., Referenceless PRF shift thermometry. Magn Reson Med, 2004. 51(6): p. 1223-31.3.
4. Butts, K., et al., Interleaved echo planar imaging on a standard MRI system. Magn Reson Med, 1994. 31(1): p. 67-72.
5. Hutchinson, E.B., M.T. Buchanan, and K. Hynynen, *Design and optimization of an aperiodic ultrasound phased array for intracavitary prostate thermal therapies*. Med Phys, 1996. 23(5): p. 767-76.
6. A. Macovski, Medical Imaging Systems, Prentice-Hall, Englewood Cliffs, NJ, 1983.
7. Parker, K.J., et al., *In-Vivo Measurements of Ultrasound Attenuation in Normal or Diseased Liver. Ultrasound in Medicine and Biology*, 1988. 14(2): p. 127-136.
8. Sapareto, S.A. and W.C. Dewey, *Thermal dose determination in cancer therapy*. Int J Radiat Oncol Biol Phys, 1984. 10(6): p. 787-800.